

ML for Computational Lithography: Practical Recipes

Youngsoo Shin
youngsoo@kaist.edu
KAIST
Daejeon 34141, Korea

CCS CONCEPTS

• Hardware → VLSI design manufacturing considerations.

KEYWORDS

Lithography, Machine learning, Mask synthesis, Lithography modeling

ACM Reference Format:

Youngsoo Shin. 2025. ML for Computational Lithography: Practical Recipes. In *30th Asia and South Pacific Design Automation Conference (ASPDAC'25)*, January 20–23, 2025, Tokyo, Japan. ACM, New York, NY, USA, 3 pages. <https://doi.org/10.1145/3658617.3703145>

1 INTRODUCTION

Optical lithography, also called photolithography, consists of two processes as shown in Figure 1: mask pattern is exposed to a light source to form a photoresist (PR) pattern during optical process; and PR pattern goes through chemical (etch) process to form the final pattern on the wafer. Computational lithography comprises mathematical and algorithmic approaches to improve the resolution attainable in these processes. Its key components are

- Modeling: models optical- and chemical-processes, which enables lithography simulation.
- Mask synthesis: includes optical proximity correction (OPC), inverse lithography technology (ILT), etch proximity correction (EPC), and assist feature (AF) design.
- Test patterns: with classification and generation.
- Hotspot: including detection and correction.

Machine learning (ML) has been applied to majority of these components since around 2010 with key motivations of: (1) ML provides higher modeling capability than traditional analytical model, and (2) many lithography applications can be considered as image recognition or image conversion, which can be handled effectively with recent ML models.

Given that some ML solutions are already provided through vendor solutions, it is about right time to address which ML-assisted lithography applications have more use cases while which are still in the stage of research.

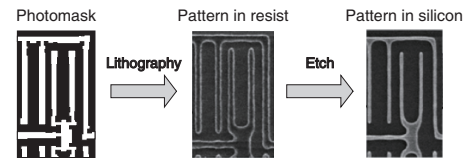


Figure 1: Optical process from mask to PR pattern, and etch process from PR pattern to wafer pattern.

2 APPLICATIONS WITH MORE USE CASES

2.1 Test Pattern Classification

Comprehensive lithography test patterns are important for lithography modeling, hotspot library, source mask optimization, and so on. Two types of test patterns are popular: parametric and actual. Parametric patterns are represented by a few geometrical parameters such as line width and space. They are easy to build and analyze, but the coverage they offer is only limited. Actual patterns are extracted from sample layouts and can cover more complex shapes. But they should be carefully classified: some patterns overlap leaving redundancies, and some are not quite important for target application, e.g. hotspot detection.

The coverage that test patterns provide, both parametric and actual, is usually not enough. ML has been applied to deliberately synthesize some new patterns, which can be added to existing parametric and actual patterns [7, 18] for higher coverage.

2.1.1 Pattern Representation. Pattern classification has relied on pattern matching: image-based, area-based, or even in frequency domain. But it is not efficient and does not entail coverage analysis. A systematic approach will rely on pattern representation, i.e. project sample patterns on a parameter space.

Image parameter space (IPS) [11], illustrated in Figure 2, consists of intensity slope (I_{slp}) at pattern edge together with maximum (I_{max}) and minimum-intensity (I_{min}) in its close proximity; it is popular in lithography modeling. IPS may be extended to include more parameters to define a higher dimensional parameter space. e.g. IPS sensitivity to geometry perturbation [14] ($\partial I_{max} / \partial M$, where M is line width). Since the choice of parameter space is only manual, alternative method is to introduce an ML model and use some model features (e.g. the outputs of last convolution layer) for parameter space [1].

IPS reflects the exposure process of optical model but does not capture post-exposure bake (PEB) and development of resist model. It has been shown that IPS together with a few Gaussian convolutions (inspired by the fact that resist signal is weighted sum of convolutions between light intensity and Gaussian kernels) can be a good representation to capture both models [2].

Permission to make digital or hard copies of all or part of this work for personal or classroom use is granted without fee provided that copies are not made or distributed for profit or commercial advantage and that copies bear this notice and the full citation on the first page. Copyrights for third-party components of this work must be honored. For all other uses, contact the owner/author(s).
ASP-DAC'25, January 20–23, 2025, Tokyo, Japan
© 2025 Copyright held by the owner/author(s).
ACM ISBN 979-8-4007-0635-6/25/01
<https://doi.org/10.1145/3658617.3703145>

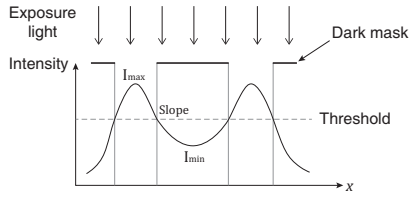


Figure 2: Image parameter space (IPS) consisting of I_{slp} , I_{max} , and I_{min} .

2.2 Etch Bias Model

During the etch process shown in Figure 1, some patterns experience over-etch due to PR erosion, which causes negative etch bias. Some others experience under-etch due to excessive deposition, causing positive etch bias. This is illustrated in Figure 3. Etch proximity correction (EPC), or retargeting, is a process to correct the PR pattern, the OPC target, in a way that such potential over- and under-etch are accounted for.

Etch bias model is a key for EPC. Rule-based (RB) or model-based (MB) models are popular. In RB, etch biases are experimentally obtained for a number of parametric patterns, and are tabulated with index of line width and spacing, for instance. In MB, regression is performed with sample etch biases while a number of empirical parameters (e.g. density kernel, visible kernel, and blocked kernel) are assumed. The regression result in analytical form is then used as MB model. Both RB and MB compact models are crude and cannot model complex chemical etch process with enough accuracy. Rigorous model also exists and is accurate but is too slow [6].

An attempt has been made to use ML model for etch bias [12], demonstrating that higher accuracy is possible even with simple multi layer perceptron (MLP). As usual, the choice of ML input parameters and the choice of network type (regression vs. classification) are important subject of engineering.

2.3 OPC and ILT

The mask synthesis is computation intensive process, so it is tempting to apply ML for speed up. The output from ML model may not be used for actual mask synthesis due to model's limited accuracy and the reliability concern on the model (if the model has not been trained well or if the model has some bugs). Realistic use case would be to consider ML output as initial mask image, which is provided to standard OPC or ILT solution. This still offers significant speed-up, e.g. about 3 times in OPC [4] process, since standard solution now can complete much earlier with less iterations.

A simple MLP still helps in quick prediction of mask bias [4], the amount of shift applied to each segment for correction. A key is to provide relevant inputs that strongly affect mask bias but are convenient to collect. Polar Fourier transform (PFT) signals, the convolutions of local patterns and optic kernel, turn out to be such inputs [3].

More complex ML models have also been studied. An example is bi-directional recurrent neural network (BRNN) [9], where a number of neural networks (NNs) are connected through intermediate layers to account for correctons in neighbor segments (mapped to neighbor NN).

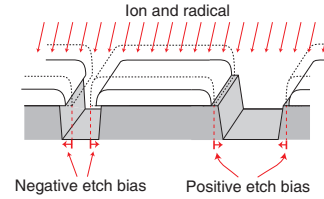


Figure 3: Etch bias: negative and positive.



Figure 4: The result of Manhattan- vs curvilinear-OPC.

Curvilinear OPC, in which each pattern segment is assumed as cubic Bézier curve instead of a line, may also benefit from ML given that curve correction is even more complex and time consuming. In addition, the amount of curvature that can reliably be transferred from mask to wafer is limited, which adds additional complexity to curvilinear OPC. ML models have been tried [8]: MLP for moving curve endpoints and graph convolutional networks (GCNs) for intermediate points. Figure 4 compares the result of standard Manhattan OPC and curvilinear OPC.

Generative adversarial Net (GAN), a popular generative ML model, has been used for quick prediction of ILT image [19].

3 APPLICATIONS STILL IN RESEARCH

3.1 Optical Model

Lithography simulation is a foundation of computational lithography. It is based on lithography model, illustrated in Figure 5, which describes the response of PR to exposure and development. Exposure is captured by optical model, in which image intensity is described by the weighted sum of convolutions between mask image $M(x, y)$ and optical kernel functions ϕ_i :

$$I(x, y) = \sum \lambda_i |\phi_i \otimes M(x, y)|^2, \quad (1)$$

where λ_i is a weight value. This method is called sum of coherent systems (SOCS) approximation [5]. Development is captured by resist model; resist signal R models PEB, which is compared to some threshold T to model development.

The conditional GAN (CGAN) has been applied to directly obtain PR contour from mask pattern so that the whole models in Figure 5 can be encapsulated within a single ML model. It has been applied to contact or via patterns, and extra CNN has also been applied to adjust the center of each pattern for higher accuracy. A complex valued neural network (CVNN) has been proposed for both optical- and resist-model [10]. The frequency components of actual patterns are usually limited, so small amount of training data can produce a model of higher accuracy in frequency domain even though there are extra processes of Fourier- and inverse Fourier-transform.

The SOCS optical model is quite efficient, in accuracy and computation time, so using ML model in its place sees less success.

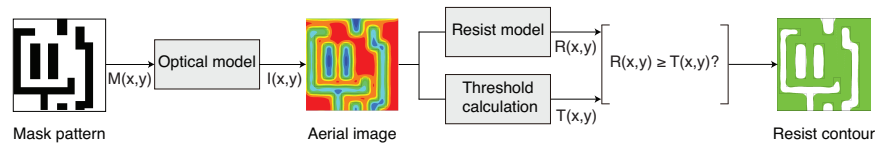


Figure 5: Lithography model.

3.2 Hotspot

Hotspot patterns are the ones that may cause defects such as bridging, necking, and line-end shortening. They can be identified through process variation band (PVB), a set of contours from repeated lithography simulation with varying lithography conditions. Such patterns are stored in hotspot library, and are used for hotspot detection through pattern matching.

Hotspot detection using CNN has been proposed [17]. Since hotspots are sparse, it is important to augment sample hotspot patterns so that CNN is well trained. A simple flipping and rotating have been tried for this purpose, even though it is still not enough. Automatic correction of hotspot using cycle-consistent GAN (cycleGAN) has also been presented [13].

There are some hurdles in applying ML to hotspot applications: (1) hotspot patterns are sparse, so it is difficult to train the ML model well, (2) the solution should be perfect, e.g. miss prediction (predict hotspot patterns as non-hotspot ones), which often occurs in ML model, is not allowed.

3.3 Assist Features

Assist feature, or sub-resolution assist feature (SRAF) or scattering bar, is a key resolution enhancement technique (RET). It is an extra pattern added to the mask, not intended to be printed on the wafer, helping nearby main patterns to be printed with higher fidelity and improved process window. As an intuitive example, sparse lines exhibit broader linewidth variations than dense lines, so adding assist features to both sides of sparse lines creates a dense environment [16].

SRAFs are usually inserted before OPC and are refined while main patterns are corrected. Deep CNN has been applied for quick prediction of SRAF guidance map (SGM) [15], which is used for SRAF insertion process; SGM value indicates the sensitivity of improving process windows on the desired pattern. Similarly, CNN has been used to predict continuous transmission mask (CTM), similar to SGM, which is used for SRAF insertion through ILT.

Recently ILT is being considered as an integrated engine for both main patterns and SRAFs, and so independent SRAF applications through ML speed-up become less appealing.

ACKNOWLEDGMENTS

The author would like to thank Dr. Seongbo Shim from Samsung for discussion.

REFERENCES

[1] K. Chen et al. 2019. Full-chip application of machine learning SRAFs on DRAM case using auto pattern selection. In *Proc. SPIE 10961, Optical Microlithography XXXII*, 1096108.

[2] G. Cho, Y. Kwon, P. Kareem, and Y. Shin. 2022. Integrated test pattern extraction and generation for accurate lithography modeling. *IEEE Tr. on Semiconductor Manufacturing* 35, 3 (Aug. 2022), 495–503.

[3] S. Choi, S. Shim, and Y. Shin. 2016. Machine learning (ML)-guided OPC using basis functions of polar Fourier transform. In *Proc. SPIE 9780, Optical Microlithography XXIX*.

[4] S. Choi, S. Shim, and Y. Shin. 2018. Neural network classifier-based OPC with imbalanced training data. *IEEE Tr. on CAD* 38, 5 (May 2018), 938–948.

[5] N. Cobb, A. Zakhor, and E. Miloslavsky. 1996. Mathematical and CAD framework for proximity correction. In *Proc. SPIE 2726, Optical Microlithography IX*.

[6] Y. Fan et al. 2017. Accurate characterization of 2D etch bias by capturing surrounding effects from resist and trench areas. In *Proc. SPIE Advanced Lithography*, Vol. 10147.

[7] P. Kareem, Y. Kwon, and Y. Shin. 2020. Layout pattern synthesis for lithography optimizations. *IEEE Tr. on Semiconductor Manufacturing* 33, 2 (May 2020), 283–290.

[8] S. Kim, G. Cho, S. Zhang, and Y. Shin. 2024. Fast and accurate curvilinear OPC with ML-guided curve correction. In *Proc. Int. SoC Design Conf.*

[9] Y. Kwon, Y. Song, and Y. Shin. 2019. Optical proximity correction using bidirectional recurrent neural network (BRNN). In *Proc. SPIE 10962, Design-Process-Technology Co-optimization for Manufacturability XIII*, 109620D.

[10] H. Lee et al. 2020. A physics-driven complex valued neural network (CVNN) model for lithographic analysis. In *Proc. SPIE 11326, Advances in Patterning Materials and Processes XXXVII*.

[11] T. Roessler, B. Frankowsky, and O. Toublan. 2003. Improvement of empirical OPC model robustness using full-chip aerial image analysis. In *Proc. SPIE 5256, 23rd Annual BACUS Symp. on Photomask Technology*, 222–229.

[12] S. Shim and Y. Shin. 2017. Machine learning-guided etch proximity correction. *IEEE Tr. on Semiconductor Manufacturing* 30, 1 (Feb. 2017), 1–7.

[13] W. Sim et al. 2019. Automatic correction of lithography hotspots with a deep generative model. In *Proc. SPIE 10961, Optical Microlithography XXXII*, 1096105.

[14] D. Vengertsev et al. 2012. The new test pattern selection method for OPC model calibration, based on the process of clustering in a hybrid space. In *Proc. SPIE 8522, Photomask Technology 2012*, 85221A. 387 – 394.

[15] S. Wang et al. 2017. Machine learning assisted SRAF placement for full chip. In *Proc. SPIE 10451, Photomask Technology 2017*, Vol. 10451. 95–101.

[16] A. Wong. 2001. *Resolution Enhancement Techniques in Optical Lithography*. SPIE press.

[17] H. Yang et al. 2017. Imbalance aware lithography hotspot detection: a deep learning approach. In *Proc. SPIE 10148, Design-Process-Technology Co-optimization for Manufacturability XI*, 1014807.

[18] H. Yang et al. 2019. DeePattern: layout pattern generation with transforming convolutional auto-encoder. In *Proc. Design Automation Conference*. ACM.

[19] H. Yang, S. Li, Y. Ma, B. Yu, and E. Young. 2018. GAN-OPC: Mask Optimization with Lithography-guided Generative Adversarial Nets. In *Proc. Design Automation Conf. (DAC)*. 1–6.